

New result on the measurement of the direct photon emission in $K^+ \rightarrow \pi^+\pi^0\gamma$ decay

M.A. Aliev^{a*}, Y. Asano^b, P. Depommier^c, M. Hasinoff^d,
 K. Horie^e, Y. Igarashi^f, J. Imazato^f, A.P. Ivashkin^a,
 M.M. Khabibullin^a, A.N. Khotjantsev^a, Y.G. Kudenko^a, G.Y. Lim^f,
 O.V. Mineev^a, J.A. Macdonald^{g†}, C. Rangacharyulu^h, S. Sawada^f, S. Shimizuⁱ

(The E470 KEK-PS Collaboration)

^a Institute for Nuclear Research RAS, Moscow, 117312 Russia

^b Institute of Applied Physics, University of Tsukuba, Ibaraki 305-0006, Japan

^c Laboratoire de Physique Nucleaire, Universite de Montreal, Montreal, Quebec, Canada H3C 3J7

^d Department of Physics and Astronomy, University of British Columbia, Vancouver, Canada V6T 1Z1

^e Research Center for Nuclear Physics, Osaka University, Ibaraki, Osaka 567-0047, Japan

^f Institute of Particle and Nuclear Studies (IPNS), High Energy Accelerator Research Organization (KEK), Ibaraki 305-0801, Japan

^g TRIUMF, Vancouver, British Columbia, Canada V6T 2A3

^h Department of Physics, University of Saskatchewan, Saskatoon, Canada S7N 5E2

ⁱ Department of Physics, Osaka University, Osaka 560-0043, Japan

Abstract

We present a new result on the $K^+ \rightarrow \pi^+\pi^0\gamma$ decay measurement using stopped kaons. The best fit to the decay spectrum comprised of 10k events gives a branching ratio for the direct photon emission of $[3.8 \pm 0.8(stat) \pm 0.7(syst)] \times 10^{-6}$ in the π^+ kinetic energy region of 55 to 90 MeV. This result has been obtained with the assumption that there is no component due to interference with the inner bremsstrahlung.

*Corresponding author. *E-mail address*: malik@inr.ru

†Deceased

1 Introduction

The chiral anomaly [1, 2] is a fundamental property of chiral quantum field theories such as the Standard Model of quantum chromodynamics (QCD). Its theoretical origin and mathematical properties are well understood, while experimental tests, which are crucial for the theoretical basis of particle physics, are relatively rare. Although the chiral anomaly can be interpreted as a short-distant effect, it manifests itself most directly in the low-energy interactions of the pseudoscalar mesons [3–6]. The chiral anomaly manifests itself also in the non-leptonic weak interactions. As already shown in Refs. [7, 8], only radiative K decays (among them $K^+ \rightarrow \pi^+\pi^0\gamma$) are sensitive to this anomaly.

The total amplitude of the $K^+ \rightarrow \pi^+\pi^0\gamma$ decay can be written as a sum of inner bremsstrahlung (IB) and direct emission (DE) amplitudes. The IB amplitude is associated with the $K^+ \rightarrow \pi^+\pi^0$ ($K_{\pi 2}$) decay, in which the photon is emitted from the outgoing π^+ , and is completely predicted by the quantum electrodynamics in terms of the $K_{\pi 2}$ amplitude [9]. The DE amplitude, in which the photon is emitted directly from one of the intermediate states of the decay, can in turn be decomposed into electric and magnetic parts.

Within the framework of Chiral Perturbation Theory (ChPT), the magnetic amplitude appears first at $O(p^4)$. There are two different ways for its manifestation: the reducible amplitude [7], which can be derived directly from the Wess-Zumino-Witten functional [6], and the direct contributions [8, 10], which are subject to some theoretical uncertainties. In both cases the direct emission amplitudes are dominated by the anomaly. For the electric amplitude there is no definite prediction from ChPT. The experimental study of the electric amplitude, which could be observed through an interference (INT) with the IB amplitude, is of high interest not only for ChPT but also for possible non-standard-model effects such as the CP-violation asymmetry between the $K^+ \rightarrow \pi^+\pi^0\gamma$ and the $K^- \rightarrow \pi^-\pi^0\gamma$ decay widths.

The remarkable feature of the $K^+ \rightarrow \pi^+\pi^0\gamma$ and the $K_L \rightarrow \pi^+\pi^-\gamma$, is that the normally dominant IB amplitude is strongly suppressed because it violates the $\Delta I=1/2$ rule. Therefore the DE amplitude is relatively enhanced. The DE component can also be isolated kinematically. These features simplify the experimental verification of the anomalous amplitude, making the $K^+ \rightarrow \pi^+\pi^0\gamma$ decay an important instrument to investigate the low energy structure of QCD.

A conventional way to express the differential decay rate of the $K^+ \rightarrow \pi^+\pi^0\gamma$ decay is to use terms of T_+ and W , where T_+ is the kinetic energy of the π^+ in the K^+ rest frame, and W is an invariant parameter defined as $W = (P \cdot q)(p_+ \cdot q)/(m_{\pi^+}^2 M_{K^+}^2)$. Here, P , p_+ and q are the 4-momenta of the K^+ , π^+ and γ , respectively. The differential decay rate can be written in terms of the IB component rate as [11]

$$\frac{\partial^2 \Gamma}{\partial T_+ \partial W} = \frac{\partial^2 \Gamma_{IB}}{\partial T_+ \partial W} \left\{ 1 + 2 \frac{m_{\pi^+}^2}{M_{K^+}} \text{Re} \left(\frac{E}{eA} \right) W^2 + \frac{m_{\pi^+}^4}{M_{K^+}^2} \left(\left| \frac{E}{eA} \right|^2 + \left| \frac{M}{eA} \right|^2 \right) W^4 \right\}, \quad (1)$$

where A is the decay amplitude for the $K^+ \rightarrow \pi^+\pi^0$, and E and M are the electric and magnetic amplitudes of the DE component, respectively.

Table 1: Summary of the previous measurements of the direct photon emission in $K^\pm \rightarrow \pi^\pm \pi^0 \gamma$ decays.

Experiment	Sort of experiment	Kaon	Number of events	$Br(DE)$
BNL 1972 [12]	in-flight	K^\pm	2100	$[1.56 \pm 0.35 \pm 0.5] \times 10^{-5}$
CERN 1976 [13]	in-flight	K^\pm	2461	$[2.3 \pm 3.2] \times 10^{-5}$
Protvino 1987 [14]	in-flight	K^-	140	$[2.05 \pm 0.46_{-0.23}^{+0.39}] \times 10^{-5}$
BNL E787 2000 [15]	stopped	K^+	2×10^4	$[4.7 \pm 0.8 \pm 0.3] \times 10^{-6}$
KEK E470 2003 [16]	stopped	K^+	4434	$[3.2 \pm 1.3 \pm 1.0] \times 10^{-6}$
Protvino 2004 [17]	in-flight	K^-	930	$[3.7 \pm 3.9 \pm 1.0] \times 10^{-6}$

The experimental status of the measurement of the DE component of the $K^+ \rightarrow \pi^+ \pi^0 \gamma$ decay is shown in Table 1. As one can see, there is a large discrepancy between the results of the first three [12–14] and the second three [15–17] experiments. These results can also be compared with corresponding theoretical predictions for the branching ratio of the DE component in the same kinetic energy region of the π^+ [7, 8, 10]. The above-mentioned situation encouraged us to perform a new analysis of the experimental data of the E470 experiment.

2 Experiment

Experiment E470 was performed at the KEK 12 GeV proton synchrotron using the E246 experimental apparatus constructed to search for T -violating transverse muon polarization in $K^+ \rightarrow \pi^0 \mu^+ \nu$ ($K_{\mu 3}$) decay [18]. In addition to the T -violation search, spectroscopic studies for various decay channels have also been successfully performed using this detector system [19]. The apparatus is shown in Fig. 1, and is described in detail elsewhere [20–23]. A separated K^+ beam ($\pi^+/K^+ \sim 7$) of 660 MeV/c was used with a typical intensity of 1.5×10^5 kaons per spill of 2 s duration with a 4 s repetition time. To distinguish K^+ 's from π^+ 's a Cherenkov counter [20] was used. A beam counter B0 [23], an assembly of 22 plastic scintillating counters, placed before the Cherenkov counter, was used to obtain the K^+ and π^+ beam profiles. Kaons were slowed down in an Al+BeO degrader, and stopped in an active target made of 256 scintillating fibers, which was located at the centre of a 12-sector superconducting toroidal spectrometer. The charged π^+ from kaon decay passed through one of the twelve fiducial (also called TOF1) counters, surrounding the target, and entered one of the spectrometer sector gaps, and was then detected by a TOF2 counter, located at the exit of the spectrometer. Tracking of charged particles and their momentum analysis was done using multi-wire proportional chambers at the entrance (C2) and exit (C3 and C4) of each magnet sector, as well as by the active target and an array of ring counters [21] surrounding the target. The energies and angles of the photons were measured by the CsI(Tl) photon calorimeter consisting of 768 CsI(Tl)

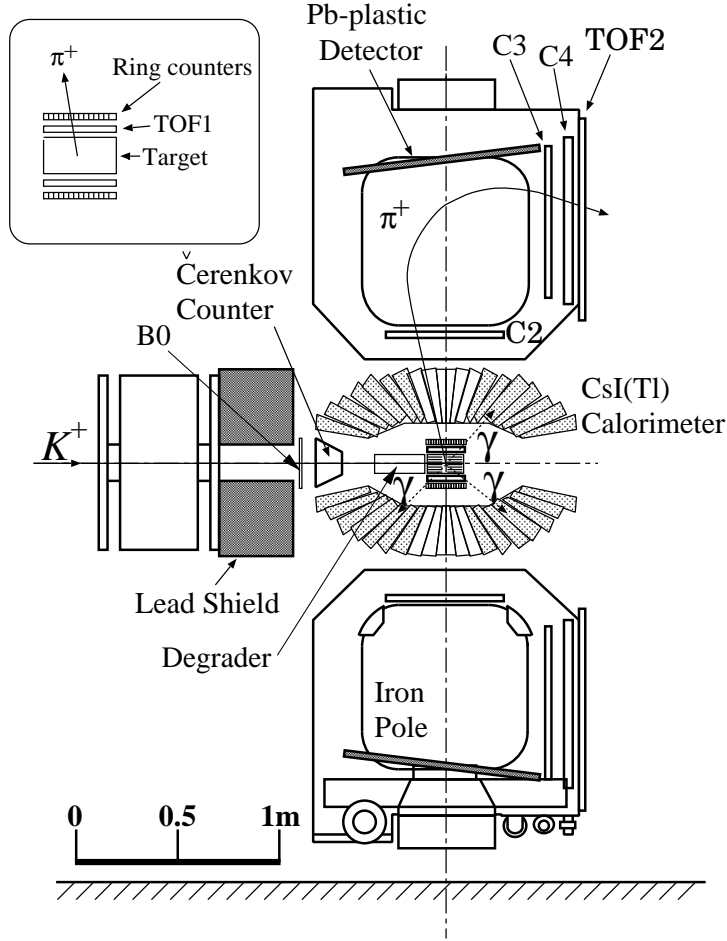


Figure 1: The layout of the detector for E470 experiment.

modules [22]. The CsI(Tl) barrel had twelve holes for the charged particle entry to the toroidal spectrometer, and covered a solid angle of about $0.75 \times 4\pi$ sr.

To collect the $K^+ \rightarrow \pi^+ \pi^0 \gamma$ data the following trigger was used

$$C_K \times [Fid_i \times TOF2_i] \times 3\gamma \times (1, 2)B0 \times (1, 2)ring,$$

where C_K is a kaon Cherenkov counter, Fid_i is a hit in the i th fiducial (TOF1) counter or in its immediate neighbors, $TOF2_i$ is a hit in the i th TOF2 counter, 3γ is 3-photon clusters in CsI(Tl) barrel, and $(1, 2)B0$ and $(1, 2)ring$ are multiplicities of the B0 counter and ring counters ≤ 2 , respectively.

3 Analysis

In this analysis we aimed to improve our previous result [16] of the measurement of the direct photon emission in $K^+ \rightarrow \pi^+\pi^0\gamma$ decay by reanalyzing the experimental data accumulated in 2001. For this purpose a new analysis strategy was adopted. This included: 1) selecting as many good $K^+ \rightarrow \pi^+\pi^0\gamma$ events as possible by imposing several loose cuts; 2) increasing the quality of data by improving the pairing efficiency of the photons from π^0 decay, and 3) improving the $K_{\pi 3}$ background rejection. The analysis strategy was carefully studied and optimized by a Monte Carlo simulation.

The decay time of the stopped K^+ in the target was defined by a signal in the TOF1 counter. To reject in-flight K^+ decays this time was required to be more than 3 ns later than the K^+ arrival time into the target.

For the analysis only events with three photon clusters in the CsI(Tl) calorimeter have been selected. This condition considerably suppresses the backgrounds from the $K_{\pi 2}$, K_{e3} , $K_{\mu 3}$ and $K_{\pi 3}$ modes, although some fraction of these events pass the trigger due to different reasons— the K_{e3} and $K_{\mu 3}$ modes due to an accidental photon hit in the CsI(Tl) calorimeter; the $K_{\pi 3}$ mode due to the escape of one photon into a CsI(Tl) calorimeter hole. The $K_{\pi 2}$ events pass through the trigger condition mostly due to identification one of the two photons from π^0 decay dissipated in two parts as two photons. As a result of such misidentification we have three photon clusters in the CsI(Tl) calorimeter instead of two.

To separate e^+ 's and μ^+ 's from π^+ 's, the squared mass of the charged particles M_{TOF}^2 was calculated using the time of flight of the charged particles from the TOF1 to the TOF2 counter, and their specific energy deposition dE/dx in the TOF2. Such separation completely remove the remaining K_{e3} background, and considerably reduced the $K_{\mu 3}$ background.

Constraints on the reconstructed K^+ mass $M_{K^+} = E_{\pi^+} + \sum_{i=1}^3 E_{\gamma_i}$ were set to be $420 < M_K < 510$ MeV/c². To set a cut on the momentum $\vec{p}_K = \vec{p}_{\pi^+} + \sum_{i=1}^3 \vec{p}_{\gamma_i}$ we used the parameter $\Delta p = \sqrt{p_x^2 + p_y^2 + p_z^2}$, where $p_\alpha = p_{\pi^+\alpha} + \sum_{i=1}^3 p_{\gamma_i\alpha}$ ($\alpha = x, y, z$), and used the condition of $\Delta p < 60$ MeV/c.

To reject in-flight decays of π^+ 's and suppress the scattering of charged particles from the magnetic pole faces, a track consistency cut $\chi^2 < 10$ has been imposed. The remaining $K_{\pi 2}$ background has been removed by requiring the π^+ momentum to be less than 180 MeV/c.

For further analysis we need to reconstruct the π^0 . Since we have three photons in the CsI(Tl), there are also three possible combinations to form the π^0 . To improve the pairing efficiency of the photons the following method was developed. The quantities $Q_{i,j}^2$ ($i, j=1,2,3$), sums of six asymmetric terms for each pair of photons comprised of the i th and j th photon, were introduced as follows:

$$Q_{i,j}^2 = \frac{(\theta_{\pi^0\gamma_{6-i-j}}^{exp} - \theta_{\pi^0\gamma})^2}{(\sigma_{\theta_{\pi^0\gamma}})^2} + \frac{(\theta_{\pi^+\gamma_{6-i-j}}^{exp} - \theta_{\pi^+\gamma})^2}{(\sigma_{\theta_{\pi^+\gamma}})^2} + \frac{(E_{\pi^0(\gamma_i\gamma_j)}^{calc0} - E_{\pi^0(\gamma_i\gamma_j)}^{calc1} - \Delta E_{\pi^0})^2}{(\sigma_{E_{\pi^0}})^2} +$$

Table 2: The values of parameters in the $Q_{i,j}^2$ expressions.

Expression	Offset	σ (Expression < 0)	σ (Expression > 0)
$E_{\gamma_{6-i-j}}^{calc} - E_{\gamma_{6-i-j}}^{exp} - \Delta E_\gamma$, MeV	$\Delta E_\gamma = 2.54$	$\sigma_{E_\gamma} = 6.25$	$\sigma_{E_\gamma} = 12.86$
$m_{\gamma_i\gamma_j} - M_{\gamma\gamma}$, MeV/c ²	$M_{\gamma\gamma} = 130.72$	$\sigma_{m_{\gamma\gamma}} = 22.05$	$\sigma_{m_{\gamma\gamma}} = 4.5$
$\theta_{\pi^0\gamma_i}^{exp} - \theta_{\pi^0\gamma}$, deg	$\theta_{\pi^0\gamma} = 107.53$	$\sigma_{\theta_{\pi^0\gamma}} = 19.52$	$\sigma_{\theta_{\pi^0\gamma}} = 17.52$
$E_{\pi^0(\gamma_i\gamma_j)}^{calc0} - E_{\pi^0(\gamma_i\gamma_j)}^{calc1} - \Delta E_{\pi^0}$, MeV	$\Delta E_{\pi^0} = -2.58$	$\sigma_{E_{\pi^0}} = 12.12$	$\sigma_{E_{\pi^0}} = 9.31$
$\theta_{\pi^+\gamma_{6-i-j}}^{exp} - \theta_{\pi^+\gamma}$, deg	$\theta_{\pi^+\gamma} = 129.18$	$\sigma_{\theta_{\pi^+\gamma}} = 32.60$	$\sigma_{\theta_{\pi^+\gamma}} = 15.10$
$\theta_{\pi^+\pi_{i,j}^0}^{exp} - \theta_{\pi^+\pi^0}$, deg	$\theta_{\pi^+\pi^0} = 150.04$	$\sigma_{\theta_{\pi^+\pi^0}} = 24.43$	$\sigma_{\theta_{\pi^+\pi^0}} = 9.67$

$$\frac{(m_{\gamma_i\gamma_j} - M_{\gamma\gamma})^2}{(\sigma_{m_{\gamma\gamma}})^2} + \frac{(E_{\gamma_{6-i-j}}^{calc} - E_{\gamma_{6-i-j}}^{exp} - \Delta E_\gamma)^2}{(\sigma_{E_\gamma})^2} + \frac{(\theta_{\pi^+\pi_{i,j}^0}^{exp} - \theta_{\pi^+\pi^0})^2}{(\sigma_{\theta_{\pi^+\pi^0}})^2}. \quad (2)$$

Here, the superscripts "exp" and "calc" stand for the experimental and calculated values, respectively. So, $E_{\pi^0(\gamma_i\gamma_j)}^{calc0}$ and $E_{\pi^0(\gamma_i\gamma_j)}^{calc1}$ are the calculated energies of the π^0 comprised of a combination of i th and j th photons, using the formulae:

$$E_{\pi^0(\gamma_i\gamma_j)}^{calc0} = \frac{\sqrt{2}m_{\pi^0}}{\sqrt{(1 - \cos \theta_{\gamma_i,\gamma_j}^{exp}) \left[1 - \left(\frac{E_{\gamma_i}^{exp} - E_{\gamma_j}^{exp}}{E_{\gamma_i}^{exp} + E_{\gamma_j}^{exp}} \right)^2 \right]}}, \quad (3)$$

$$E_{\pi^0(\gamma_i\gamma_j)}^{calc1} = \frac{M_{K^+}^2 + m_{\pi^0}^2 - m_{\pi^+}^2}{2M_{K^+}} - \frac{2E_{\gamma_{6-i-j}}^{exp} (E_{\pi^+}^{exp} - P_{\pi^+}^{exp} \cos \theta_{\pi^+\gamma_{6-i-j}}^{exp})}{2M_{K^+}}. \quad (4)$$

$E_{\gamma_{6-i-j}}^{calc}$, the energy of the $(6 - i - j)$ th photon (supposing it is the unpaired one), is calculated from the following formula:

$$E_{\gamma_{6-i-j}}^{calc} = \frac{(M_K^2 + m_{\pi^+}^2 - m_{\pi^0}^2 - 2M_K E_{\pi^+}^{exp})}{2(M_K - E_{\pi^+}^{exp} + p_{\pi^+}^{exp} \cos \theta_{\pi^+\gamma_{6-i-j}}^{exp})}. \quad (5)$$

$m_{\gamma_i\gamma_j} = \sqrt{2E_i^{exp} E_j^{exp} (1 - \cos \theta_{\gamma_i\gamma_j}^{exp})}$ is the invariant mass of the (i, j) photon combination. Other parameters in the $Q_{i,j}^2$ expressions, which were obtained using MC simulation, are given in Table 2.

Since the distribution of the expressions in parentheses of each term's numerator in (2) is asymmetrical, the root mean square (σ) corresponding to each term has two values, one corresponding to the expression being < 0 , and the other to the expression being > 0 . At this stage the variables of $Q_{i,j}$ have been optimized to maximize the pairing efficiency of the DE component using the MC simulation, which we obtained to be 88%. For the IB component we obtained 70% efficiency. Sub-indexes of the minimum $Q_{i,j}$ are accepted to be the indexes of the two photons, which come from the π^0 . We number all three photons

in the following way: the most energetic photon from the π^0 decay is ascribed the number 1, the lower energetic photon is labeled by 2. We ascribe number 3 to the third unpaired photon.

At the second stage we represent the events in a scatterplot as shown in Fig. 2.

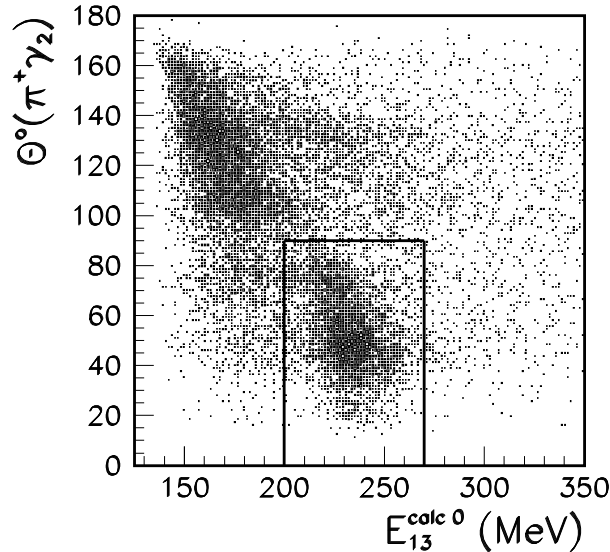


Figure 2: Scatterplot of $\theta_{\pi+\gamma_2}$ vs E_{13}^{calc0} . Here, $\theta_{\pi+\gamma_2}$ is the opening angle between π^+ and γ_2 , and E_{13}^{calc0} is the parameter $E_{\pi^0(\gamma_i\gamma_j)}^{calc0}$ with $i = 1, j = 3$. The detached region is a region of incorrect photons pairing.

As the MC simulation shows the region in the rectangular box is a region of photons mispairing. Namely, for these events the γ_2 doesn't really come from the π^0 decay but is the unpaired one. Consequently the γ_3 is actually the lower energy photon from the π^0 decay. In order to determine the true combination of the photons in the detached region as well, we renumber the events in this region as follows: we ascribe number two to the third photon and number three to the second one. Such simple cross-renumbering of events allowed us to enhance the pairing efficiency of the IB component up to 93%, although the DE component was reduced down to 81%. Nevertheless, on the whole we increased the pairing efficiency considerably, and this in turn reduced the systematic error associated with mispairing. For comparison, in the previous analysis [16] the pairing efficiencies were 85% and 79% for IB and DE components, respectively.

The K_{π_3} background was rejected by a 2-dimensional cut as shown in Fig. 3. Such a cut not only allowed us to successfully reject this mode but also saved good $K^+ \rightarrow \pi^+\pi^0\gamma$ events in the π^+ low momentum region.

The total number of good $K^+ \rightarrow \pi^+\pi^0\gamma$ events in the π^+ momentum region of 115 to 180 MeV/c, obtained after applying the above selection criteria, is 10,154, which is about 2.3 times higher than in the previous analysis [16]. The background from K_{π_3} decay has been estimated to be less than 0.2% by the simulation. In the previous analysis the

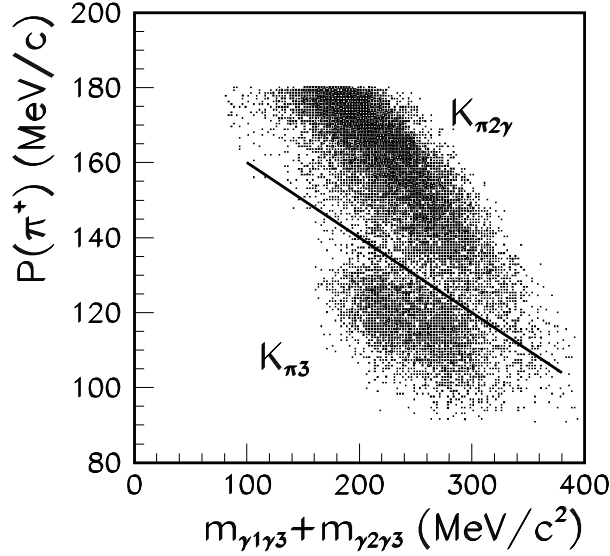


Figure 3: Scatterplot of the π^+ momentum versus the sum of "invariant masses" comprised of γ_1, γ_3 and of γ_2, γ_3 . The shown line is a cut condition to remove the $K_{\pi 3}$.

contribution of this mode was about 1.2%.

A MC simulation of the $K_{\pi 3}$ decay was used to test the simulation of the experiment. The matrix element of $K_{\pi 3}$ decay for this simulation was taken from the PDG [24]. In the simulation, the form factors of the $K_{\pi 3}$ matrix element were taken to be the world average quoted by the PDG [24]. In this analysis we selected events with 4 photon clusters in the Cs(Tl) using the following conditions, $P_{\pi^+} < 135$ MeV/c, $14000 < (M_{\pi^+}^{tof})^2 < 25000$ (MeV/c²)², $\Delta p < 80$ MeV/c, $380 < M_K < 520$ MeV/c², $80 < E_{\pi_1^0} < 200$ MeV, $60 < E_{\pi_2^0} < 190$ MeV, $60 < m_{(\gamma\gamma)1} < 150$ MeV/c², $55 < m_{(\gamma\gamma)2} < 150$ MeV/c². Various $K_{\pi 3}$ spectra are shown in Figs. 4, 5, and we see excellent agreement between the experimental data and the MC simulation.

A MC simulation of the $K_{\pi 2\gamma}$ decay was carried out for both the IB and the DE components of the $K_{\pi 2\gamma}$ decay, using the matrix elements given in [25]. The detector acceptances for the IB and the DE components have been obtained to be $\Omega(IB) = 0.566 \times 10^{-3}$ and $\Omega(DE) = 1.659 \times 10^{-3}$. Figure 6 shows the $K^+ \rightarrow \pi^+ \pi^0 \gamma$ spectra, which have been obtained after imposing an additional cut of $W < 0.5$ in order to remove the DE component. Again we find very good agreement between the experiment and the MC simulation.

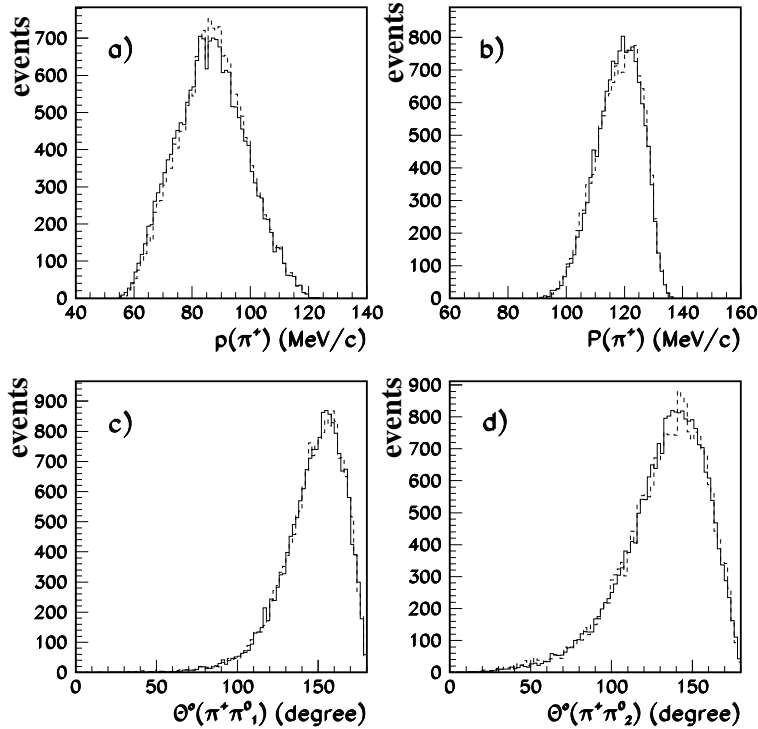


Figure 4: $K_{\pi 3}$ spectra: a) - π^+ momentum before correction for energy losses in the target; b) - π^+ momentum after correction for energy losses in the target. c) - opening angle between π^+ and π_1^0 ; d) - opening angle between π^+ and π_2^0 . The solid lines are the experimental data and the dashed lines are the MC predictions.

4 Results

The fraction of the DE component in the selected $K^+ \rightarrow \pi^+\pi^0\gamma$ events has been obtained by fitting the experimental data distribution of $\theta_{\pi^+\pi^0}$, E_γ and W in 3-D space with a sum of IB and DE components obtained from the MC simulation. The Maximum log-likelihood method has been used for fitting the χ^2 defined as follows

$$\chi^2 = 2 \sum [y_i - n_i + n_i \ln(n_i/y_i)], \quad (6)$$

where $y_i = A \times (y_i^{IB} + \alpha y_i^{DE})$. Here, n_i is the number of real data in the i -th bin of the histogram, and y_i^{IB} , y_i^{DE} are numbers of MC data of IB and DE components in the same i -th bin of the histogram, respectively. The variable α is the fraction of the DE component normalized to the IB one and A is a normalizing coefficient. The MINUIT package was used to obtain the minimum of χ^2 . The error values correspond to shifts of the variables, which increased the χ^2 by 1. The value of α was obtained to be 0.026 ± 0.006 with a

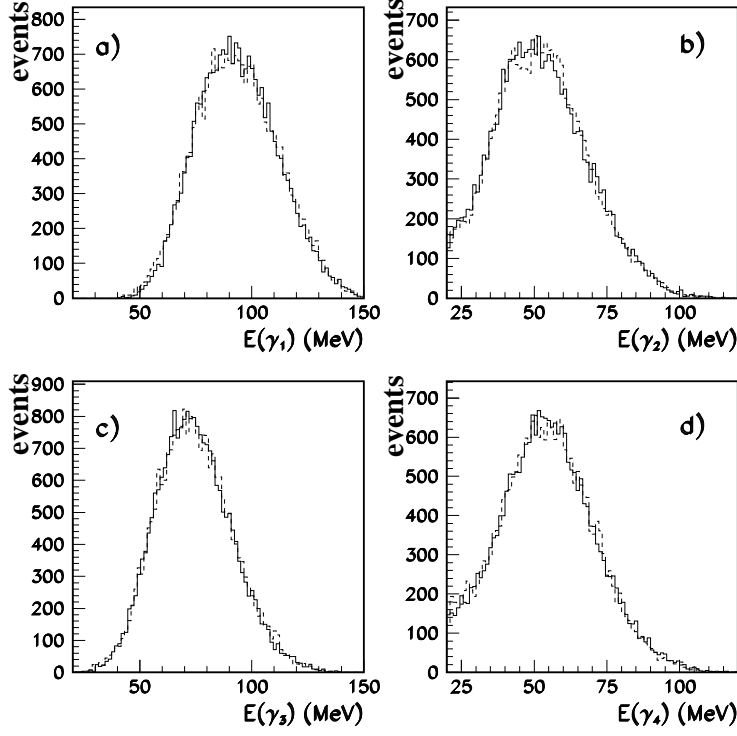


Figure 5: Spectra of $K_{\pi 3}$: a) - energy of $E_{\gamma 1}$; b) - energy of $E_{\gamma 2}$; c) - energy of $E_{\gamma 3}$; d) - energy of $E_{\gamma 4}$. The solid lines are the experimental data and the dashed lines are the MC predictions.

$\chi^2/ndf=1.15$. The experimental spectrum of W normalized to the pure IB component is shown in Fig. 7. The obtained branching ratio of the DE component in the π^+ kinetic energy region of 55 to 90 MeV is $Br(DE) = [3.8 \pm 0.8(stat)] \times 10^{-6}$.

The major systematic errors come from the uncertainty of the CsI(Tl) calorimeter calibration, γ mispairing effect, accidental background, the spectrometer field uncertainty, and also from the uncertainty of the kaon stopping x, y position.

The uncertainty due to the γ calibration of the CsI(Tl) calorimeter was estimated by changing the value of the DE branching ratio by the maximum shift of the calibration coefficients of the CsI(Tl) calorimeter. The corresponding shift of the DE branching ratio obtained in this way was $\pm 0.5 \times 10^{-6}$. The γ mispairing effect was studied by changing the pairing efficiency of the photons along with a change of the selection cuts. The shift of the DE branching ratio as a result of such changes was $\pm 0.4 \times 10^{-6}$. The uncertainty from the accidental background, mainly associated with the $K_{\mu 3}$ decay, was estimated by varying the TDC gate widths, and was found to be less than 7% of the DE branching ratio value, that is $\pm 0.3 \times 10^{-6}$. The error due to the spectrometer field uncertainty

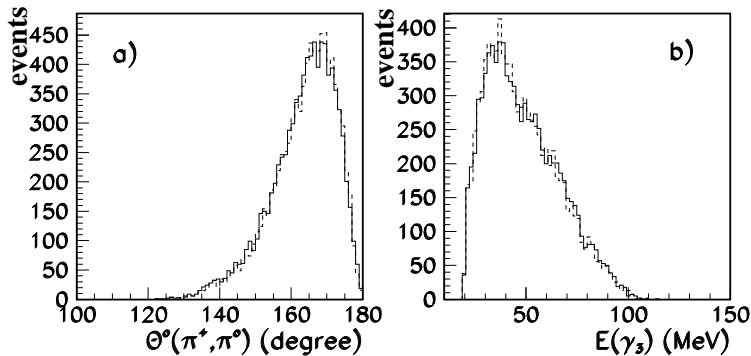


Figure 6: Spectra of $K^+ \rightarrow \pi^+\pi^0\gamma$ with an additional cut of $W < 0.5$. a) opening angle between the π^+ and the π^0 ; b) energy of γ_3 . The solid lines are the experimental data and the dashed lines are the IB component from the Monte Carlo predictions.

($\pm 0.1 \times 10^{-6}$) was evaluated by shifting the field strength by $\pm 0.2\%$. The error due to the uncertainty in the reconstruction of the kaon stopping x , y position was studied by a shift of the kaon stopping point along the charged pion track by one fiber which corresponds to 5 mm. The resulting variation of the DE branching ratio was $\pm 0.2 \times 10^{-6}$. All the uncertainties are summarized in Table 3.

Table 3: Summary of the systematic errors.

ERROR SOURCE	UNCERTAINTY, $\Delta Br(DE) \times 10^6$
γ calibration	0.5
γ mispairing	0.4
Accidental background	0.3
Spectrometer field uncertainty	0.1
Kaon stopping x , y coordinates	0.2
Total systematic error	0.7

5 Conclusion

We have obtained an improved result for the branching ratio of direct photon emission in the $K^+ \rightarrow \pi^+\pi^0\gamma$ decay from the analysis of the E470 data. We have extracted 10154 $K^+ \rightarrow \pi^+\pi^0\gamma$ events in the π^+ momentum region of 115 to 180 MeV/c, which is about 2.3 times more than in the previous analysis [16]. In addition to a reduction of the statistical error we have also reduced the systematic error by increasing the pairing efficiency of the

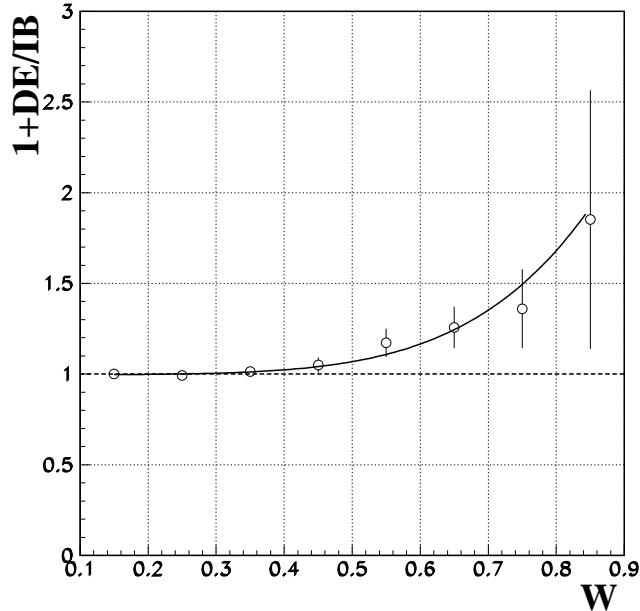


Figure 7: W spectrum of the observed $K^+ \rightarrow \pi^+\pi^0\gamma$ events normalized to the IB component obtained from the Monte Carlo simulation. The solid curve shows the best fit of the W spectrum to a sum of the IB and DE components.

photons. The optimization of the selection cuts allowed us to increase the total number of the extracted $K^+ \rightarrow \pi^+\pi^0\gamma$ events, and to obtain more sensitivity to the DE component part of the $K^+ \rightarrow \pi^+\pi^0\gamma$ spectrum. In this analysis we have provided more efficient rejection of the $K_{\pi 3}$ background, which was estimated by MC simulation to be less than 0.2% as compared to 1.2% in the previous analysis.

The branching ratio for the DE component in the π^+ kinetic energy region 55 to 90 MeV has been determined to be

$$Br(DE) = [3.8 \pm 0.8(stat) \pm 0.7(syst)] \times 10^{-6},$$

which is consistent with the results of the three last experiments [15–17]. The good agreement of this result with the theoretical prediction for the branching ratio of the DE component, $Br(DE) = 3.5 \times 10^{-6}$ [7, 8], supports the hypothesis that the dominant contribution to direct photon emission is due to the pure magnetic transition given by the reducible anomalous amplitude. It should also be stressed that the result has been obtained with the assumption that the INT component is zero.

Acknowledgments. This work has been supported in Japan by a Grant-in-Aid from the Ministry of Education, Science, Sports and Culture, and by JSPS; in Russia by the Ministry of Education and Science; in Canada by NSERC and IPP, and by the TRIUMF infrastructure

support provided under its NRC contribution. The authors gratefully acknowledge the excellent support received from the KEK staff.

References

- [1] S.L. Adler, Phys. Rev. **177** (1969) 2426; J.S. Bell and R. Jackiw, Nuovo Cim. **A 60** (1969) 47; W.A. Bardeen, Phys. Rev. **184** (1969) 1848.
- [2] S.L. Adler, arXiv:hep-th/0411038.
- [3] S. Weinberg, Physica **A 96** (1979) 327.
- [4] J. Gasser and H. Leutwyler, Annals Phys. **158** (1984) 142.
- [5] J. Gasser and H. Leutwyler, Nucl. Phys. **B 250** (1985) 465.
- [6] J. Wess and B. Zumino, Phys. Lett. **B 37** (1971) 95; E. Witten, Nucl. Phys. **B 223** (1983) 422.
- [7] G. Ecker, H. Neufeld and A. Pich, Phys. Lett. **B 278** (1992) 337.
- [8] J. Bijnens, G. Ecker and A. Pich, Phys. Lett. **B 286** (1992) 341 [arXiv:hep-ph/9205210].
- [9] F.E. Low, Phys. Rev. **110** (1958) 974.
- [10] H.-Y. Cheng, Phys. Rev. **D 42** (1990) 72.
- [11] G. D'Ambrosio, G. Isidori Z. Phys. **C 65** (1995) 649 [arXiv:hep-ph/9408219].
- [12] R.J. Abrams *et al.*, Phys. Rev. Lett. **29** (1972) 1118.
- [13] K.M. Smith *et al.*, Nucl. Phys. **B 109** (1976) 173.
- [14] V.N. Bolotov *et al.*, Yad. Fiz. **45** (1987) 1652.
- [15] S.C. Adler *et al.* [E787 Collaboration], Phys. Rev. Lett. **85** (2000) 4856 [arXiv:hep-ex/0007021].
- [16] M.A. Aliev *et al.* [KEK-E470 Collaboration], Phys. Lett. **B 554** (2003) 7 [arXiv:hep-ex/0212048].
- [17] V.A. Uvarov *et al.*, arXiv:hep-ex/0410049.
- [18] M. Abe *et al.* [KEK-E246 Collaboration], Phys. Rev. Lett. **83** (1999) 4253; M. Abe *et al.* [KEK-E246 Collaboration], Phys. Rev. Lett. **93** (2004) 131601 [arXiv:hep-ex/0408042].

- [19] S. Shimizu *et al.*, Phys. Lett. **B 495** (2000) 33; K. Horie *et al.*, Phys. Lett. **B 513** (2001) 311; S. Shimizu *et al.*, Phys. Rev. **D 70** (2004) 037101; A.S. Levchenko, *et al.*, Phys. Atom. Nucl. **65** (2002) 2232.
- [20] M.P. Grigorev *et al.*, Instrum. Exp. Tech. **41** (1998) 803.
- [21] A.P. Ivashkin *et al.*, Nucl. Instrum. Meth. **A 394** (1997) 321.
- [22] A.D. Dementjev *et al.*, Nucl. Instr. and Meth. **A 440** (2000) 151-171.
- [23] J.A. Macdonald *et al.* [E246 KEK PS Collaboration], Nucl. Instrum. Meth. **A 506** (2003) 60 [arXiv:hep-ex/0302001].
- [24] S. Eidelman *et al.*, Particle Data Group Collaboration, Phys. Lett. **B592** (2004).
- [25] G. Ecker, H. Neufeld and A. Pich, Nucl. Phys. **B 413** (1994) 321 [arXiv:hep-ph/9307285].